Mechanism and Action of Myotoxin *A* from a Rattlesnake Venom

ANTHONY T. Tu
Department of Biochemistry & Molecular Biology Colorado State University, Fort Collins, Colorado 80523, USA

Myonecrosis

Myonecrosis, or muscle damage, is one of the common pathologic symptoms induced by snake envenomation, especially from snakes in the families Crotalidae and Viperidae (Fig. 1). There are several types of snake venom proteins that produce myonecrosis. One group includes molecularly small nonenzymatic proteins, such as myotoxin *a* and its analogues with a molecular weight of roughly 5000. The second type, with M_rs of 12,000-16,000, includes myotoxic phospholipases A. The third type includes hemorrhagic toxins that produce myonecrosis. The fourth type includes miscellaneous compounds that are also myonecrotic. For instance, *C. durissus terrificus* venom is well known to be neurotoxic, but it also is myonecrotic [1].

As with hemorrhagic toxins, venom usually contains multiple myonecrotizing components [2a,b]. Because some components are not uniformly present in all venoms, it is not surprising that the early stage of myopathogenesis is especially venom dependent. At a later stage, damaged muscle will reach the same pathological endpoint, regardless of the variety of venom (Fig. 2).

Myotoxin a

Among different myotoxins, myotoxin *a* was the first one isolated in pure form and is still the one best studied [3,4]. Myotoxin *a* is isolated from the venom of *C. viridis viridis* (prairie rattlesnake). Its primary

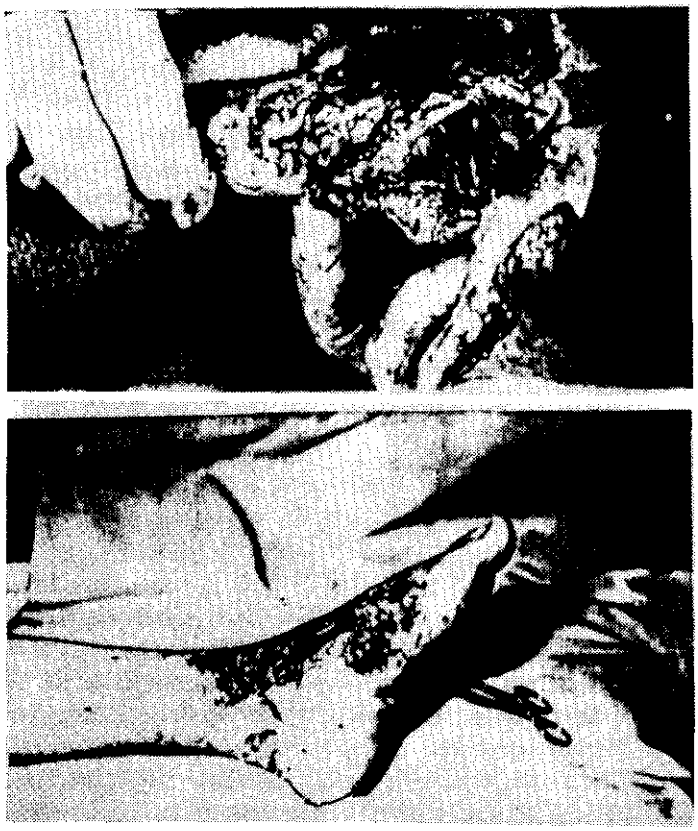

Fig. 1. Example of rattlesnake bites. Notice severe tissue damage on hand (top photo) and on leg (lower photo).

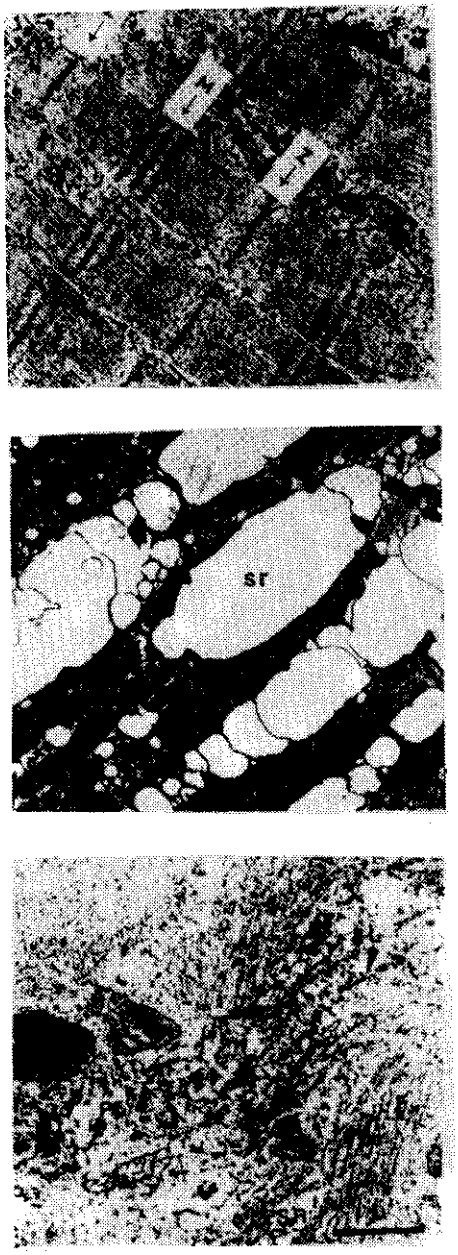

Fig. 2. Top: Electronmicrograph of normal muscle. Middle: Early stage of the muscle after injection of myotoxin *a* or by crude venom of *Crotalus viridis viridis*. Note the swelling of sarcoplasmic reticulum (SR). Lower: Degenerate muscle after injection of myotoxin *a* or crude venom. Note the disappearance of regular organization of myosin and active fibrils. The muscle becomes amorphorus.

structure has 42 amino acid residues with three disulfide bonds (Fig. 3).

The presence of a myotoxin-like molecule is common among Crotalidae venoms (Fig. 4). For instance, *C. viridis concolor* venom contained two myotoxin *a*-like molecules designated myotoxin I and myotoxin II [5]. An extensive study was made by Bober *et al.*, [6] for the presence of myotoxin *a*-like protein in 95 venoms of the genera *Agkistrodon*, *Bitis*, *Bothrops*, *Calloselasma*, *Crotalus*, *Sistrurus*, *Naja*, and *Vipera*. This investigation used both immunodiffusion and enzyme-linked immunosor-bent assay (ELISA) techniques, and only *Crotalus* and *Sistrurus* venoms contained detectable amounts of myotoxin *a*-like protein.

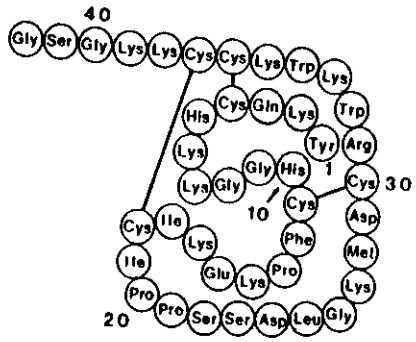

Fig. 3. Complete primary structure of myotoxin *a* with three disulfide bonds.

Attachment to Sarcoplasmic Reticulum (SR)

Electronmicroscopic observation (Fig. 2, center) indicated that myotoxin *a* caused extensive swelling of the sarcoplasmic reticulum followed by disorganization of the sarcomers. Using peroxidase-conjugated myotoxin *a*, it was found that myotoxin *a* attached to the SR membrane (Fig. 5). It was thus suggested that the attachment of the toxin to the SR is the first step in myonecrosis induced by myotoxin *a* [7].

Inhibition of Calcium Ion Loading in SR

Myotoxin *a* inhibited Ca^{2+} loading and stimulated Ca^{2+}-dependent ATPase without affecting unidirectional Ca^{2+} efflux. Its action was dose, time, and temperature dependent [8]. Myotoxin *a* partially blocked the binding of specific anti-(rabbit SR Ca^{2+}-ATPase) antibodies. It is concluded that myotoxin *a*

Sequence

	5				10				15				20				25				30				35				40				45
Myotoxin a	Y	K	Q	C	H	K	K	G	G	H	C	F	P	K	E	E	I	C	I	P	P	S	S	D	L	G	K	M	D	C	R	W	K	W	K	C	C	K	K	G	S	G		
Myotoxin I	Y	K	R	C	H	K	K	E	G	H	C	F	P	K	T	V	I	C	L	P	P	S	S	D	F	G	K	M	D	C	R	W	K	W	K	C	C	K	K	G	D	S	G	S	V A
Myotoxin II	Y	K	R	C	H	K	K	G	G	H	C	F	P	K	E	K L V	I L	C	T	P	P	S	S	D	F	G	K	M	D	C	R	-	-	-	-	-	-	-	-	D	S	G	S	V A
Peptide C	Y	K	R	C	H	K	K	G	G	H	C	F	P	K	T	V	I	C	L	P	P	S	S	D	F	G	K	M	D	C	R	W	K	W	K	C	C	K	K	G	S	V	N	
Crotamine	Y	L	Q	C	H	K	K	G	G	H	C	F	P	K	E	K	I	C	L	P	P	S	S	D	F	G	K	M	D	C	R	W	R	W	K	C	C	K	K	G	S	G		

Fig. 4. Myotoxin *a* and related myotoxic polypeptide toxins.

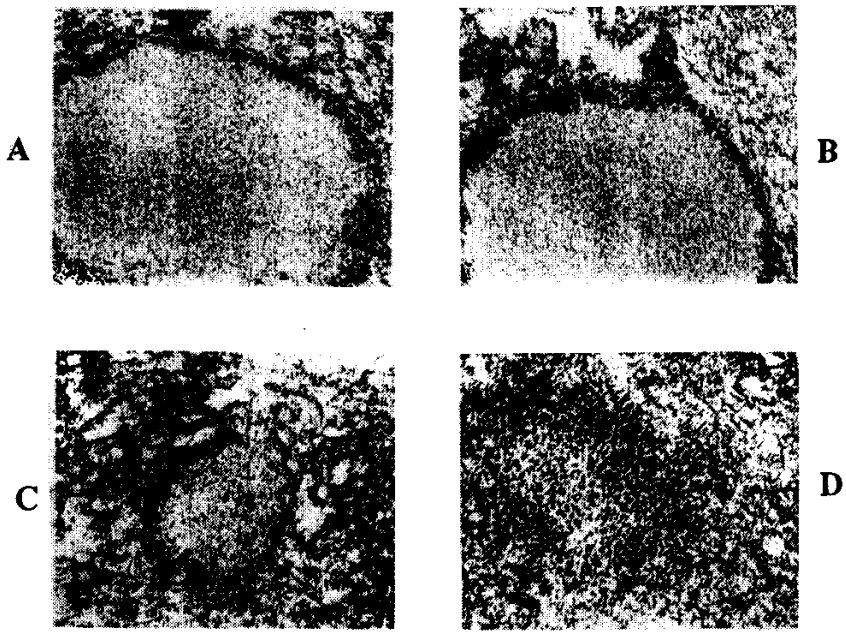

Fig. 5. Localization of horseradish peroxidase conjugated myotoxin *a*. Initial attachment of myotoxin *a* on the SR membranes (A, B, and C) and the presence of myotoxin *a* in the lumen of SR or the top of SR (D). Photographs were originally published in *Br. J. Exp. Path.* **64**, 633 (1983).

attaches to the SR Ca^{2+}-ATPase and uncouples Ca^{2+} uptake from Ca^{2+}-dependent ATP hydrolysis (Fig. 6). Myotoxin *a* also prevented the formation of decavanadate-induced two-dimensional crystalline arrays of the SR Ca^{2+}-ATPase (Fig. 7). Decavanadate induces Ca^{2+}-ATPase crystallizes only when the ATPase is in the E_2 conformation. Inhibition of crystal formation by myotoxin *a* is because myotoxin *a* binds to the Ca^{2+}-ATPase E_2 conformation, thereby preventing transition to the crystal-forming E_2 conformation.

Binding of Myotoxin a to SR Proteins

Two SR proteins bind to myotoxin *a* using a photoaffinity cross-linking agent, HSAB (*N*-hydroxy-succinimidyl 4-azidobenzoate) [9] (Fig. 8) shows the autoradiograph from SDS-PAGE of cross-linking experiments with SR proteins. In lane 1, ^{125}I-myotoxin *a* was cross-linked to proteins in whole SR vesicles. Two radiolabeled bands can be seen with apparent molecular weights of 110 K and 57 K (Fig. 8a,b). Unbound ^{125}I-myotoxin *a* can be seen in Fig. 1c.

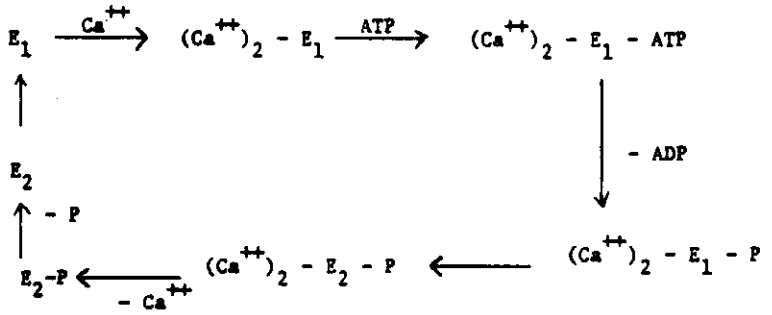

Fig. 6. Mechanism of calcium ion loading in SR involving Ca^{++}-ATPase, ATP, and calcium ion. E_1 is the Ca^{++} binding form of Ca^{++}-ATPase and E_2 is the Ca^{++} releasing form of the Ca^{++}-ATPase.

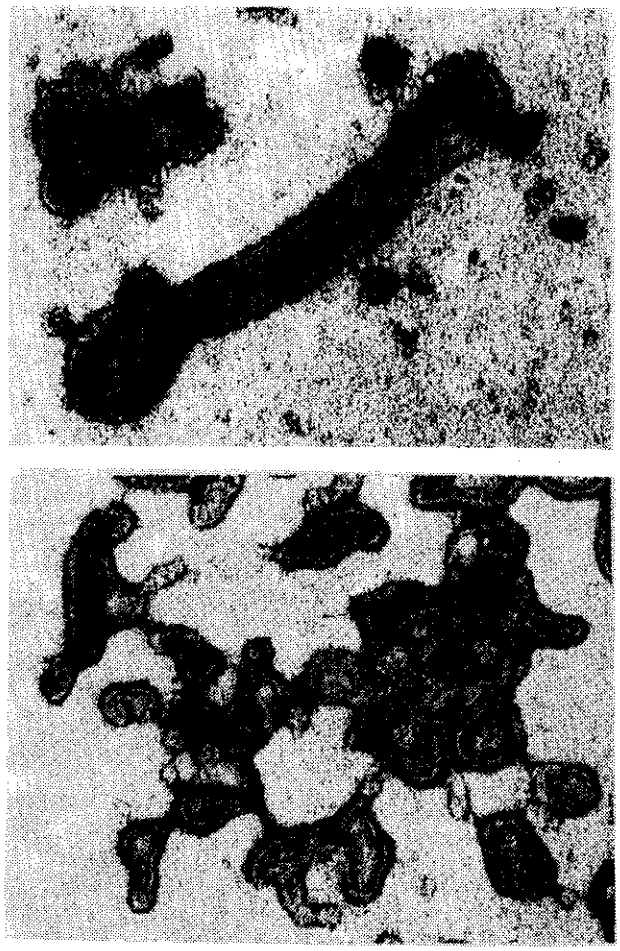

Fig. 7. Top: Two-dimensional crystal formation of SR Ca^{++}-ATPase. Only the E_2 form of the enzyme form produces such crystal. Bottom: Preincubation of Ca^{++}-ATPase with myotoxin *a* prevents the formation of crystal, indicating that myotoxin *a* attaches to the E_2 form of Ca^{++}-ATPase.

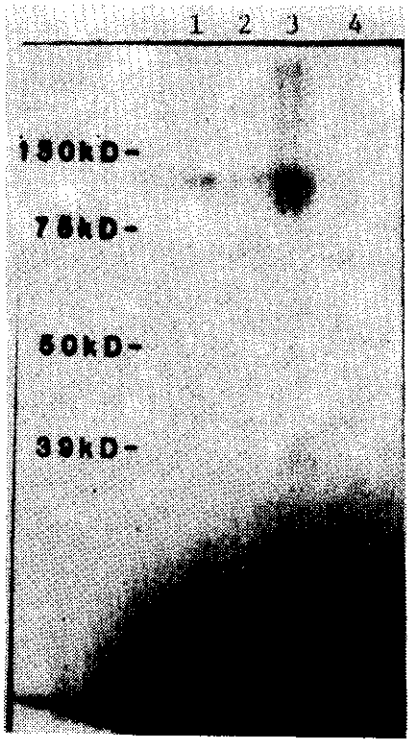

Fig. 8. Binding of ^{125}I-myotoxin *a* to two SR components (Lane 1). The addition of non-radioactive myotoxin *a* competes with ^{125}I-myotoxin *a* for the attachments (Lane 2). The addition of cobra neurotoxin does not replace the ^{125}I-myotoxin *a* attached to the SR proteins (Lane 3). Incubation of ^{125}I-cobra neurotoxin does not produce the attachments to the SR proteins (Lane 4).

Addition of nonradiolabeled myotoxin *a* to the incubation mixture containing ^{125}I-myotoxin *a* with SR proteins resulted in a decrease in the intensity of the two corresponding bands (Fig. 8, lane 2). The addition of

cobra neurotoxin as a negative control to the reaction mixture containing ^{125}I-myotoxin *a* and SR proteins did not decrease the intensity of the two bands (Fig. 8, lane 3). When ^{125}I-labeled cobra neurotoxin was incubated with SR proteins, no radioactive bands were seen on the gel (Fig. 8, lane 4).

Binding of Myotoxin a to Ca^{++}-ATPase

The 110 K band is similar to the known molecular weight of Ca^{2+}-ATPase. Therefore, the enzyme was isolated, and its affinity for myotoxin *a* was investigated. Figure 9 shows an autoradiograph of an SDS-PAGE of cross-linking experiments with purified Ca^{2+}-ATPase. Lane 1 shows the results of cross-linking the SR with ^{125}I-myotoxin *a*. Two protein bands are visible on the gel at 110 and at 57 kDa. Lane 2 shows the results of incubating ^{125}I-myotoxin *a* with Ca^{2+}-ATPase. One radioactive band is seen on the gel. Lane 3 shows the results of incubating ^{125}I-myotoxin *a* with native myotoxin *a* and Ca^{2+}-ATPase. The relative density of the one band is greatly decreased compared to lane 2. Lane 4 shows the results of the addition of cobra neurotoxin to the incubation mixture of ^{125}I-myotoxin *a* and Ca^{2+}-ATPase. One radioactive band is seen. Lane 5 shows the results of incubating ^{125}I-labeled cobra neurotoxin with Ca^{2+}-ATPase. No radioactive bands can be seen on the gel [9].

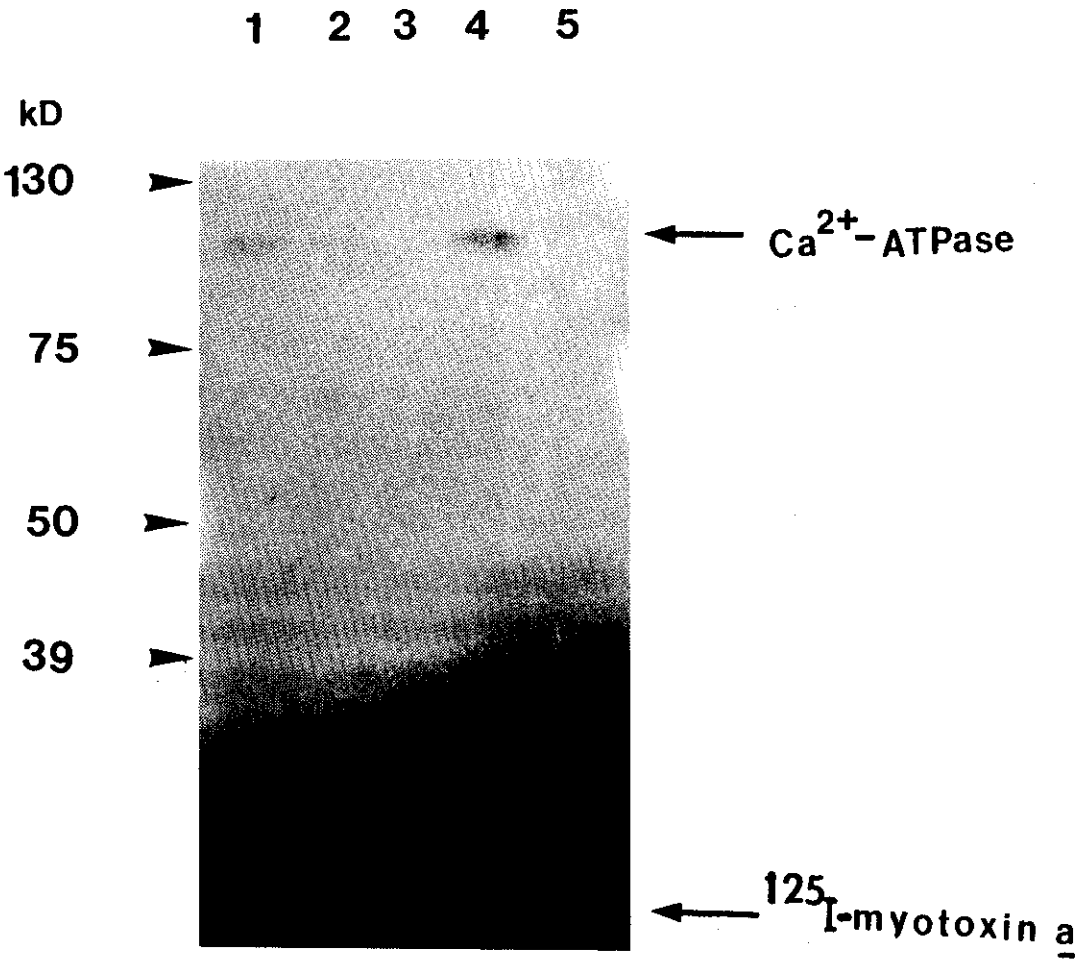

Fig. 9. Specific binding of myotoxin *a* to Ca^{++}-ATPase. Lane 1 - SR control (SR + myotoxin *a*) gives two bands. Lane 2 - Purified Ca^{2+}-ATPase + myotoxin *a* gives one band. Lane 3 - Cold myotoxin *a* replaces ^{125}I-myotoxin *a*. Lane 4 - The addition of cobra neurotoxin does not replace ^{125}I-myotoxin a already attached to Ca^{2+}-ATPase.Lane 5 - ^{125}I-cobra neurotoxin does not attach to Ca^{2+}-ATPase.

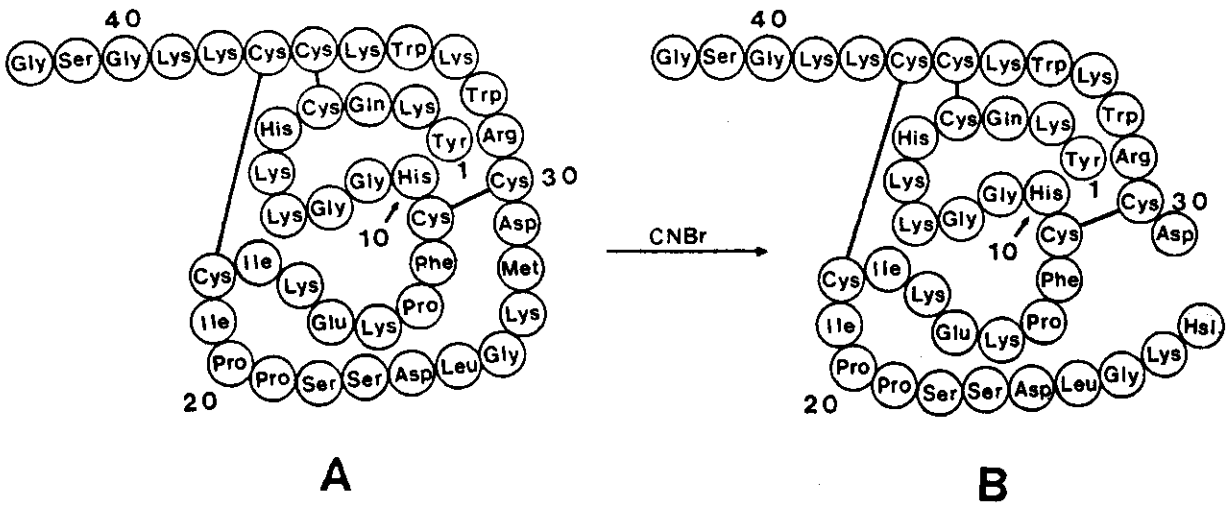

Fig. 10. Formation of nicked myotoxin *a* with CNBr.

Structure-Function Relationship

A. Aromatic Side Chain

Aromatic side-chain interactions in proteins provide an important mechanism of intermolecular binding, specificity, and recognition. In order to examine the microenvironment of the aromatic residue, CIDNP spectroscopy (photochemically induced dynamic nuclear polarization) was used [10].

The upfield shift of His_5 (both the 4 and 2 protons) and of proton C(2) of His_{10} is the result of the diamagnetic shielding of Tyr_1, due to the aromatic interaction between Tyr_1 and His_5 (as well as His_{10}).

In addition to the above diamagnetic shielding, the observation of two different line-broadening effects in the CIDNP and NMR spectra of the aromatic protons of myotoxin *a* should be taken as an indication of side-chain interaction within the Tyr_1-His_5-His_{10} aromatic cluster.

B. Nicked Myotoxin a

Myotoxin *a* can be nicked at Met_{28} by cyanogen bromide producing a unique molecule of the nicked myotoxin *a* (Fig. 10). Judging from circular dichroism, the nicked myotoxin *a* had a conformation similar to that of original myotoxin [11]. Raman spectra indicated that the conformations of the three disulfide bonds were not affected in nicked myotoxin *a* (Fig. 11). Like the original toxin, nicked myotoxin *a* was myotoxic and inhibited calcium ion loading activity, although the inhibitory action was slightly lower than that of the original myotoxin *a*. Both modified and unmodified myotoxin *a* showed myonecrotic activity as determined by examining histological slides. The modified toxin also inhibited the formation of decavanadate-induced two-dimensional crystalline arrays of the sarcoplasmic reticulum Ca^{2+}-ATPase just as the original myotoxin *a* does.

Comparison to Crotamine

Myotoxin *a* is a myotoxic protein isolated from *Crotalus viridis viridis* venom from North America. During the characterization of myotoxin *a*. We noticed some similarities [12]. There are only three residues difference (Fig. 4). These are:

Myotoxin *a*	Crotamine
Ile (19)	Leu
Leu (25)	Phe
Lys (33)	Arg

The CD spectra of two related toxins are also very similar (Fig. 12). The original paper on crotamine [13] did not mention myonecrotic activity. However, subsequent study by Cameron and Tu [12] indicated that crotamine produced necrosis in the muscle just like myotoxin *a*.

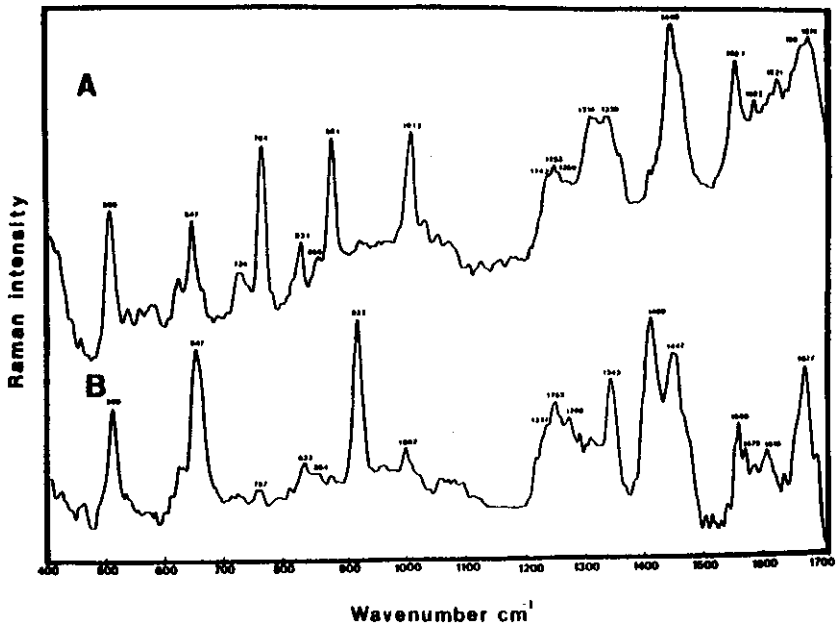

Fig. 11. Laser Raman spectra of myotoxin *a* (A) and nicked myotoxin *a* (B). Note the amide I band (1674 cm^{-1} for A and 1677 cm^{-1} for B) and S-S stretching vibrational band (508 for A and 509 cm^{-1} for B) are almost identical for the two compounds, indicating that myotoxin *a* and nicked myotoxin *a* have almost identical peptide backbone conformation and disulfide bond conformation.

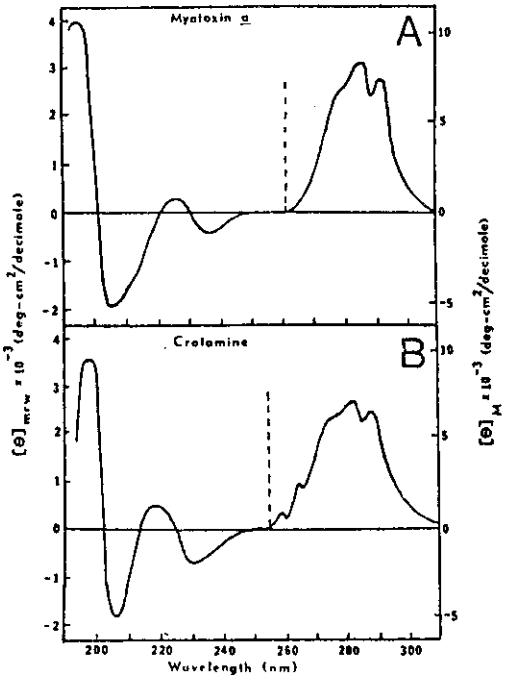

Fig. 12. Similarity of CD spectra of myotoxin *a* and crotamine.

Cloning of Myotoxin a

A. Venom Glands

A mature, individual *C. viridis viridis* was collected near Ault, Colorado. Its venom glands were removed four days after venom extraction, as the highest mRNA concentration in the venom glands of the snakes *Echis carinatus* and *Vipera palestinae* occurs after this period of time.

B. cDNA Libraries

cDNA libraries were constructed from mRNA. First, degenerated primers were used for making a cDNA fragment encoded for myotoxin *a*. Degenerated primers used are shown here:

Primer Pool N

Amino Acid Sequence	H	C	F	P	K	E	K
Oligo Sequence	CAT	TGT	TTT	CCA	AAA	GAA	A
	C	C	C	C	G	G	
			G				
			T				

Primer Pool C

Amino Acid Sequence	G	K	K	C	C	W	K
Oligo Sequence	CCT	TTT	TTA	CAA	CAT	TCC	A
	C	C	G	G	C		

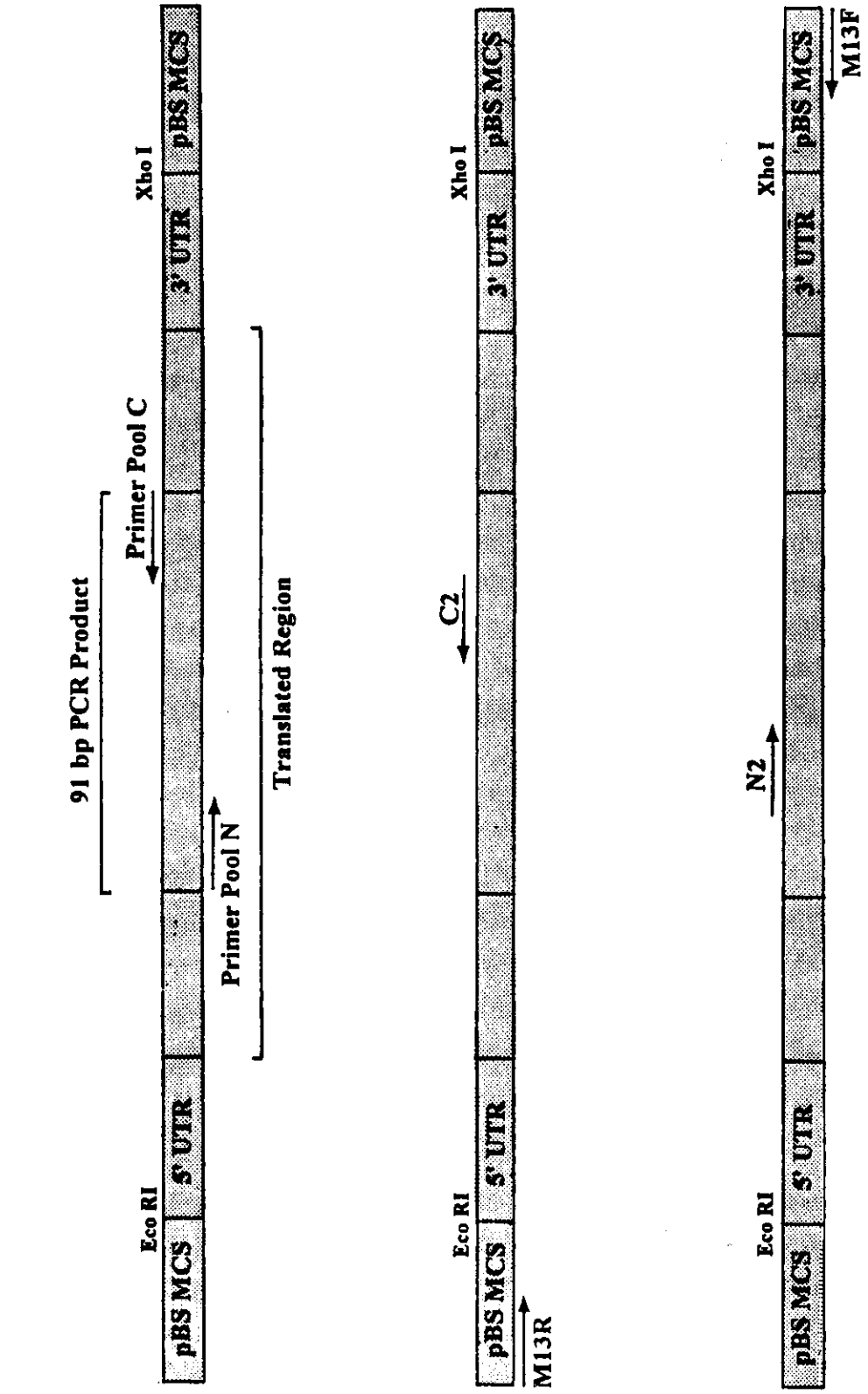

Fig. 13. Cloning Strategy. This is a diagram of the pBluescript multicloning site (pBS MCS) with the myotoxin *a* cDNA cloned between the Eco RI and Xho I restriction sites. A) Primer Pool C and Primer Pool N were used to amplify a 91 bp fragment of the myotoxin *a* translated region. B) Primer C2 and Primer M13 Reverse (M13R) were used to amplify a portion of the myotoxin *a* cDNA which includes5' UTR. C) Primer N2 and Primer M13 Forward (-20) (M13F) were used to amplify a portion of the myotoxin *a* cDNA which includes the 3' UTR.

```
                          10          20          30
PCR 1      : CGGCAGGAGCTCAGC ATG AAG ATC CTT TAT CTG CTG TTC
PCR 2      :
AMINO ACID:                      Met Lys Ile  Leu Tyr Leu Leu Phe

             40          50          60          70
PCR 1      : GCA TTT CTT TTC CTT GCA TTC CTG TCT GAA CCA GGG AAT
PCR 2      :
AMINO ACID: Ala Phe Leu Phe Leu Ala Phe Leu Ser Glu Pro Gly Asn

             80          90          100         110
PCR 1      : GCC TAT AAA CAG TGT CAG AAG AAA GGA GGA CAC TGC
PCR 2      :
AMINO ACID: Ala Tyr Lys Gln Cys His Lys Lys Gly Gly His Cys

                    120         130         140         150
PCR 1      : TTT CCC AAG GAG AAA ATA TGT ATT CCT CCA TCT TCT GAC
PCR 2      :                   AAA ATA TGT ATT CCT CCA TCT TCT GAC
AMINO ACID: Phe Pro Lys Glu Lys Ile Cys Ile Pro Pro Ser Ser Asp

                    160         170         180
PCR 1      : CTT GGG AAG ATG GAC TGT CGA TGG AAA
PCR 2      : CTT GGG AAG ATG GAC TGT CGA TGG AAA TGG AAA TGC
AMINO ACID: Phe Gly Lys Met Asp Cys Arg Trp Lys Trp Lys Cys

             190         200         210         220
PCR 1      :
PCR 2      : TGT AAA AAG GGA AGT GGA AAA TAA TGCCATCTCCATCTA
AMINO ACID: Cys Lys Lys Gly Ser Gly Lys Stop


             230         240         250         260
PCR 1      :
PCR 2      : GGACCATGGATATCTTCAAGATATGGCCAAGGACCTGAGAGT
AMINO ACID:

             271  280         290         300         310
PCR 1      :
PCR 2      : GCCGGTGCTATTGCCTTTATCTTTCTTTATCTAAATAAAATTG
AMINO ACID:

                    320
PCR 1      :
PCR 2      : CTACCTATC poly(A)
AMINO ACID:
```

Fig. 14. Complete nucleotide sequence of cDNA and the corresponding amino acid sequence of myotoxin *a*.

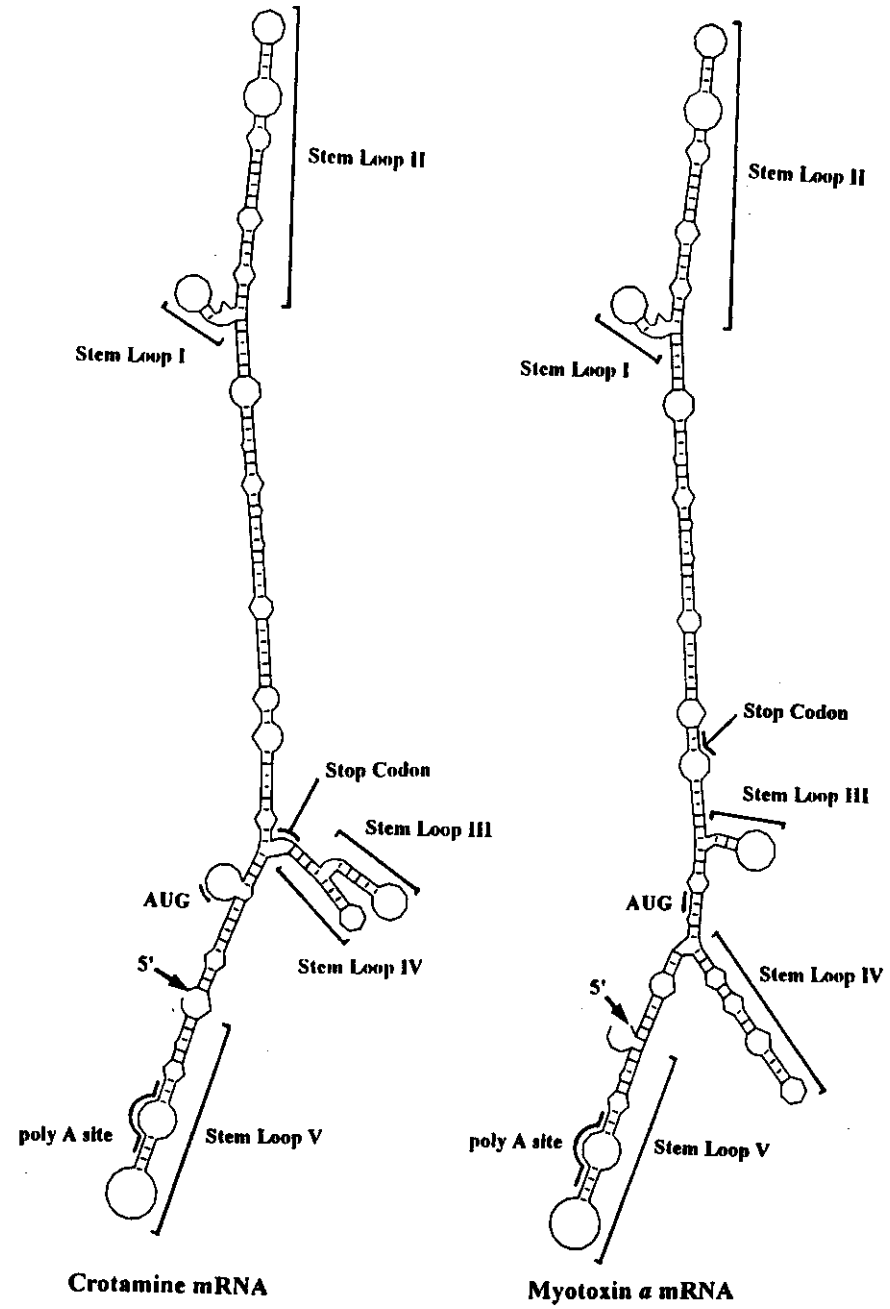

Fig. 15. Predicted secondary structure of crotamine mRNA and myotoxin *a* mRNA.

After obtaining the nucleotide sequence of the cDNA fragment, nondegenerated primers were used to construct the cDNA encoding for the whole myotoxin *a* (Fig. 13). Nondegenerated primers used are:

Primer C2

TTTCCATCGACAGTCCA

Primer N2

AAATATGTATTCCTCCATC

C. Nucleotide Sequence

The complete base sequence of a cDNA corresponding to an mRNA encoding myotoxin *a* was

determined (Fig. 14). The 5' untranslated region has 15 nucleotides, while the 3' untranslated region has 109 nucleotides. The translated portion of the myotoxin *a* cDNA encodes a start methionine, a signal peptide, the myotoxin *a* peptide sequence, and an additional lysine residue. It is likely that myotoxin *a* is secreted as the cDNA encodes a signal peptide immediately 5' to the myotoxin *a* peptide code [14].

D. Prediction of mRNA Secondary Structure

Although the secondary structures of proteins are commonly predicted, those of nucleic acids have not been extensively explored. [15] used the method of Zukker and Steigler to determine the secondary structure of mRNA's encoding phospholipase A_2 toxins from *Trimeresurus flavovoridis* (Habu snake). Further, they suggested that stem loops in the untranslated regions of these toxins may alter the translation rate or stability of snake toxin mRNA's. We also used the method of Zukker and Steigler to determine a secondary structure for the myotoxin a mRNA (Fig. 15). There are two major differences between the myotoxin *a* mRNA secondary structure and the phospholipase A_2 mRNA secondary structures. First, the coding region of the phospholipase A_2 encoding mRNA's does not participate in secondary structure formation. However, the secondary structure predicted for the myotoxin *a* mRNA is very different as the coding region does participate as part of the structure. Second, there are no stem loop structures shared by the mRNA's encoding myotoxin *a* and the phospholipase A_2 toxins.

Acknowledgements

The work has been done by many of my students, postdoctoral workers, and outside collaborators. I am deeply thankful to Mr. Mike Stringer, Dr. Charlotte Ownby, Dr. David Cameron, Dr. Jay Fox, Dr. M. Elzinga, Dr. M. Morita, Dr. N. Mori, Dr. P. Volpe, Dr. E. Damiani, Dr. A. Maurer, Dr. P. Utaisincharoen, Dr. Brenda Baker, and Mr. Jeff Norris.

References

1. M. M. Azevedo-Marques, S. E. Hering, and P. Cupo, *Toxicon*, **25**, 1163 (1987).
2. (a) C. L. Ownby, and T. T Colberg, *Toxicon*, **25**, 1329 (1987).
   (b) C. L. Ownby, and T. T Colberg,. *Toxicon*, *26*, 459 (1988).
3. D. L. Cameron, and A.T. Tu, *Biochemistry*, **16**, 2546 (1977).
4. J. W. Fox, M. Elzinga, and A. T. Tu, *Biochemistry*, **18**, 678 (1979).
5. A. L. Bieber, R. H. McFarland, and R.R. Becker, *Toxicon*, **25**, 677 (1987).
6. M. A. Bober, and C. L. Ownby, *Clin. Tox.*, **26**, 303 (1988).
7. A. T. Tu, and M. Morita, *Br. J. Exp. Pathol.* **64**, 633 (1983).
8. P. Volpe, E. Damiani, A. Maurer, and A. T Tu,. *Arch. Biochem. Biophys.* **246**, 90 (1986).
9. P. Utaisincharoen, B. Baker, and A. T. Tu, *Biochemistry*, 30, 8211 (1991).
10. K. A. Muszkat, V. Preygerzon, and A. T. Tu, *J. Prot. Chem.*, **13**, 333 (1994).
11. N. Mori, A. T. Tu, and A. Maurer, *Arch. Biochem. Biophys.* **266**, 171 (1988).
12. D. L. Cameron, and A. T. Tu, *Biochim. Biophys. Acta*, **532**, 147 (1978).
13. J. M. Gonçalves, and A. Polson, *Arch. Biochem.*, **13**, 253 (1947).
14. J. Norris, and A. T. Tu, Unpublished data (1997).
15. T. Ogawa, N. Oda, K. Nakashima, H. Sasaki, M. Hattori, Y. Sakaki, H. Kihara, and M. Ohno, *Proc. Nat. Acad. Sci. USA 89*, 8557 (1992).